Journal of Materials and Environmental Science
ISSN : 2028-2508
CODEN : JMESCN

J. Mater. Environ. Sci., 2021, Volume 12, Issue 9, Page 1176-1190

http://www.jmaterenvironsci.com

Performance of Thermally Activated Laterite on Phosphate Adsorption from Aqueous Solution: a SEM Imaging Investigation

L. S. Coulibaly[1]*, D. Sangaré[1], J. A. Mbey[2], V. B. S. Kouassi[3], L. Coulibaly [3]

[1]*UFR - Ingénierie Agronomique, Forestière et Environnementale, Département Environnement et Développement Durable, Université de Man, BP 20 Man, Côte d'Ivoire.*

[2]*University of Yaoundé 1, Laboratory of applied Inorganic Chemistry, P.O. Box 812 Yaoundé – Cameroon*

[2]*Unité de Biotechnologie et Ingénierie de l'Environnement, Unité de Formation et de Recherche en Sciences et Gestion de l'Environnement (UFR-SGE) Université Nangui Abrogoua, 02 BP 801 Abidjan 02, Abidjan, Côte d'Ivoire*

**Email address: sandotin.coulibaly@univ-man.edu.ci*

Received 10 Aug 2021,
Revised 27 Sept 2021,
Accepted 28 Sept 2021

Keywords
- ✓ *Phosphate*
- ✓ Adsorption,
- ✓ Laterite,
- ✓ Thermal activation,
- ✓ Water.

sandotin.coulibaly@univ-man.edu.ci Phone: +225 07 78 19 62 61;

Abstract

Laterite available in developing countries, have great potential for wastewater treatment. In this study, heat treated laterites from Ivory Coast (Africa) were used to remove phosphorus from water by adsorption. Microstructural properties were investigated by Scanning Electron Microscopy (SEM) and X-Ray powder Diffraction (XRD), whereas thermal properties were evaluated. Batch tests were used to evaluate adsorption capacities. X-ray Absorption Spectroscopy and SEM data evidence changes in the chemical and structural environments of the most performed heat laterite for phosphate adsorption. Thermal activation effect on laterite shows an intensification of the red colouring of the laterite and mass losses during heating. The optimal retention conditions were evaluated with four heat-treated laterites at (300; 500; 700 and 900°C). The optimal dose is 5 g/L for L-300, 7.5 g/L for L-500, L-700, and 15 g/L for L-900. The Balance Time is 6 h for L-300, 8 h for L-500, and L-700 and 12 h for L-900. The optimal pH occurs at 2 for the four thermally activated materials. Under these optimal conditions, the adsorption rate is 100, 92, 84 and 74% respectively for the laterite treated at 300, 500, 700 and 900°C respectively. Laterite treated at 300°C have the best retention capacity. The changes observed on the chemical composition and structural environments of laterite heat at 300°C could indicate these performances.

1. Introduction

The improvement in the socio-economic situation of many people is due to the expansion of agricultural and industrial production. However, some of the activities associated with the expansion adversely affected soil and water quality, affecting the health and quality of life of people and the environment. The generation of wastewater has dramatically increased the pressure on the natural environment and resulted in changes in the composition of freshwater resources [1]. This wastewater contains particularly increased levels of contaminants, in particular organic compounds of heavy metals and nutrients (phosphorus, nitrogen), which disrupt the natural balance of aquatic ecosystems [2]. The Ebrié lagoon in Abidjan is an example of such a perturbation, which is sue to the discharge of untreated domestic wastewater that considerably accelerated the eutrophication phenomenon. Additionally, in surface waters, increased nutrient levels lead to excessive growth of aquatic weeds and algae (phytoplankton). This increased production of aquatic plants has several consequences on water use [3]. Although nitrogen (N) and phosphorus (P) are considered to be the limiting nutrients for eutrophication, some algae are effective in fixing atmospheric nitrogen and, therefore, P often becomes the potentially limiting

nutrient in freshwater [4]. Excessive concentrations of phosphate in water are shown to be the main cause of eutrophication [5, 6, 7]. Consequently, the elimination of phosphates from domestic effluents is an imperative point to ensure in order to avoid the accelerated eutrophication of water bodies. Phosphates removal from wastewater can be achieved by several methods, among which adsorption appears to be of interest due to the possibility of phosphate recovery, and its inexpensive nature.
In our previous studies, laterite was used to remove phosphate from water and the percent removal achieved was high (88 %) [8]. However, although, geomaterials are known as good adsorbent for phosphate elimination, adsorption capacity can be improved by activation from several processes such as heat treatment [9], alkaline treatment [10], and acidification [11]. Heat treatment has proven to be more suitable among the activation methods mentioned above, due to its fairly simple application, its inexpensive nature with less impact on the environment [12]. This work aims to investigate the influence of the thermal treatment on the removal of P from water. To this end, raw laterite was activated at four different temperatures. The adsorption kinetics and equilibrium of phosphate frequently found in domestic wastewater were explored using these activated laterites as adsorbent. The relationships between the adsorption capacities and the structural changes occurring in the morphology and mineralogy of the natural laterite during calcination is analyzed.

2. Methodology

2.1 Materials

The raw laterite used in this research is natural material collected at Sinématialy, north of the Ivory Coast. The laterite samples directly collected in the form of blocks were washed and then dried in open air. The raw laterite powder was obtained by grinding laterite blocks using the crusher. Then crushed material is sieved to pass through an 80 µm mesh sieve. The raw laterite powder obtained is called L-raw.

2.2 Experiments

2.2.1 Preparation and characterization of activated laterite

The thermally treated samples were obtained by firing for 2 hours at temperature of 300, 500, 700 and 900 °C the raw sample (L-raw) using a Nabertherm oven, at a heating rate of 10° C.min^{-1}. Each treated sample is encoded L-X, with X being the temperature of thermal treatment. The oven was allowed to cool down to the room temperature before the heated sample is recovered and stored in polyethylene bags prior to their use. The bulk chemical composition of L-raw and activated laterite was obtained by X-Ray Fluorescence analysis using a HORIBA, MESA-50 apparatus. The mineralogical analysis was performed by X-ray diffraction (XRD) method. For thermal analysis, a LINSEIS (model STA PT-1000) apparatus, was used for TGA-DSC data acquisition.

2.2.2 Batch test: Phosphate retention study

The phosphate solution was made by dissolving K_2HPO_4 in tap water.

- ***Adsorbent dosage and pH effect***

The Adsorption tests were carried out by shaking 40 ml of phosphate solution of 2.5-10 mg / L containing 1-10 g of laterite. The solid phase was separate from the liquid through centrifugation using a Heraeus SEPATECH operating at 21.859 g. The liquid phase in further filtered using a 0.45 µm Wathman filter

and the residual phosphate concentration was measured according to the Blanchet and Malaprade method [13]. The measurements were carried out using a UV-VIS spectrometer (DR 6000). The removal of P and the adsorption capacity of the materials were determined respectively according to equations (1) and (2):

$$P_{ads}(\%) = \frac{C_0 - C_e}{C_0} . 100 \qquad \textbf{(Eqn. 1)}$$

$$q_t = \frac{(C_0 - C_t) . V}{m} \qquad \textbf{(Eqn. 2)}$$

Where C_0 is the initial concentration (mg/L) of P, q_t (mg P /g) the adsorption capacity after a shaking time t, C_t the phosphate concentration at time t (mg/L), *m* (g) the mass of the adsorbent and V(L) the volume of the solution in L.

To study the influence of pH on adsorption, the pH of the solutions was carefully adjusted between 2 and 10 by adding aquolit of 0.1 M solution of either hydrochloric acid or sodium hydroxide. The pH measurement was made with a PHYWE pH meter (Cobra 4 Sensor-Unit Chemistry).

- ***Kinetic study***

The kinetic adsorption experiment was performed in 250 mL flasks with 40 mL phosphate solution and 0.6 g adsorbents. The kinetic were evaluated at three initial phosphate concentrations (2.5; 5; 10 mg/L). The flasks were stirred at 25ºC for 168 h at 100 rpm. After each specific adsorption time, 1 mL sample was taken and then centrifuged at 5000 rpm for 10 min. Phosphate concentration of supernatant was measured as above

2.2.3 Simulation of adsorption kinetics

Pseudo-First-Order and Pseudo-Second-Order models have been adopted. The formalisms are respectively represented by **Eqn 3** and **4**:

$$log(q_e - q_t) = log(q_e) - \frac{k_1}{(2{,}303)}\, t \qquad \textbf{(Eqn. 3)}$$

$$\frac{t}{q_t} = \frac{1}{k_2 . q_e^2} + \frac{t}{q_e} \qquad \textbf{(Eqn. 4)}$$

Where q_t is the quantity of solute adsorbed at time t, q_e is the quantity of solute adsorbed at equilibrium, k_1 is the kinetic constant of the pseudo-first-order model and k_2 is the kinetic constant of the pseudo-second-order model.

3. Results and Discussion

3.1 Characterization of thermal activated laterite samples

- ***X-ray fluorescence analysis (XRF) of thermally treated laterite***

Figure 1 presents the variation curves of the proportions of Fe_2O_3, Al_2O_3, Mn_2O_3, CaO, K_2O as a function of the calcination temperature. The increase in the proportion of hematite in the samples analyzed would indicate that, there is formation of new hematite molecules (Fe_2O_3). [9] in their study on the effects of temperature on goethite, observed from 250°C to 300°C a gradual loss of hydroxyl groups of goethite which marks the start of the transformation of goethite into hematite. Also, according

to [14], the calcination of laterite at a temperature between 400°C and 800°C reveals new hematite molecules following the transformation of magnetite (Fe_3O_4). The proportion of aluminum oxide in the samples increases. It could be due to the dehydration of gibbsite (Al $(OH)_3$) giving rise to boehmite (AlOOH). This transformation was observed between 200°C and 400°C by [15]. Above 560°C, boehmite begins its conversion to alumina (γ-Al_2O_3) by dehydroxylation [16, 17] which results in an increase in the Al_2O_3 proportion. Under the influence of temperature, the mass fraction of Mn_2O_3 of the raw laterite decreases considerably from 2.36% to 0.07% when the calcination temperature reaches 300°C. This could be due to the reduction of Mn_2O_3 to Mn_3O_4. According to [18], the reduction of Mn_2O_3 to Mn_3O_4 occurs between 25°C and 1100°C. The proportion of CaO increases in the samples as the calcination temperature increases. The transformation of calcite ($CaCO_3$) into CaO would be the reason for this increase. Indeed, Sakai & Koga assert in their various works that calcium carbonate ($CaCO_3$) decomposes into lime (CaO) and carbon dioxide (CO_2) around 600°C[19, 20]. In addition, the drop in the rate of K_2O can be explained by its melting, which occurs at 350 ° C as mentioned above.

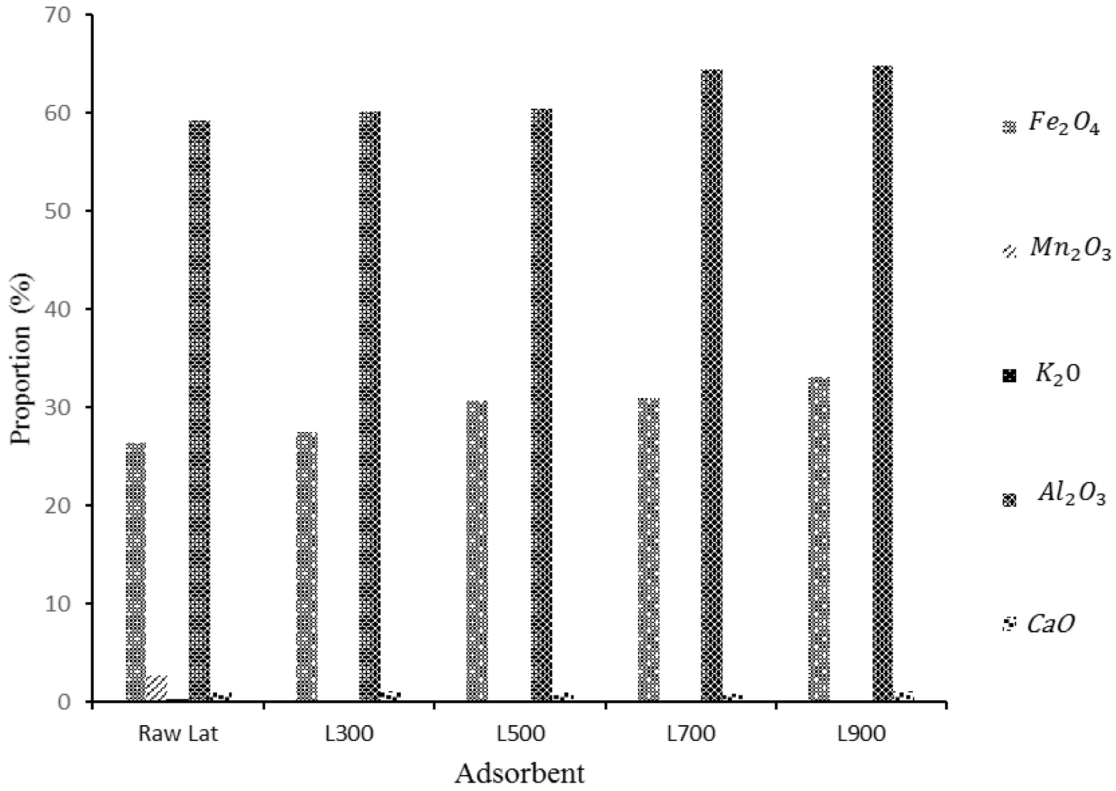

Figure 1. Variation of Fe_2O_3, Al_2O_3, Mn_2O_3, CaO, K_2O proportions as a function of the calcination temperature

– ***Mineralogical Characterization and thermal analysis***

The X-ray diffractometry analysis of raw laterite and thermally treated laterite (at 300°C) is shown in **Figure 2**. Likewise, the results of thermogravimetric analysis (TGA) and differential scanning calorimetry (DSC) at varying temperatures are shown in **Figure 3**. The mineralogical analysis of the raw laterite reveals the presence of quartz, kaolinite, goethite, and hematite. Its mineralogy could be linked to its genesis, since the laterite from Côte d'Ivoire arose from the weathering of granite and phylliths. Moreover, the XRD pattern of the calcined laterite reveals that upon a thermal treatment, the disappearance of some peaks of the gibbsite picks. This result can be explained by the transformation of the gibbsite into boehmite (Al $(OH)_3$ into α-Al_2O_3) as showed by [21]. Also, the disappearance of some

peaks of kaolinite observed. This result suggests that dehydroxylation of kaolinite occurs, and lead to the formation of metakaolinite [22]. The TGA-DSC of laterite has 3 large areas of distinct mass loss and endothermic peaks (**Figure 3**). A loss of mass of the order of 1.44% marked by endothermic peaks occurs around 45 °C. The second weight loss is 4.05% at 267°C. And the third mass loss is 5.10 % with an endothermic peak observed around 493°C. These temperature variations cause structural modifications of kaolinite contained in the laterite.

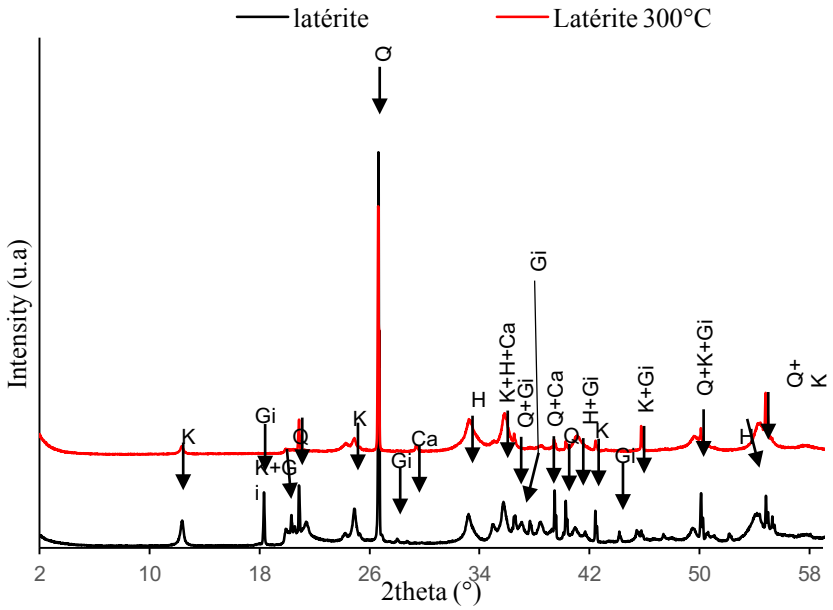

Figure 2. XRD patterns of raw laterite and heated laterite at 300°C.

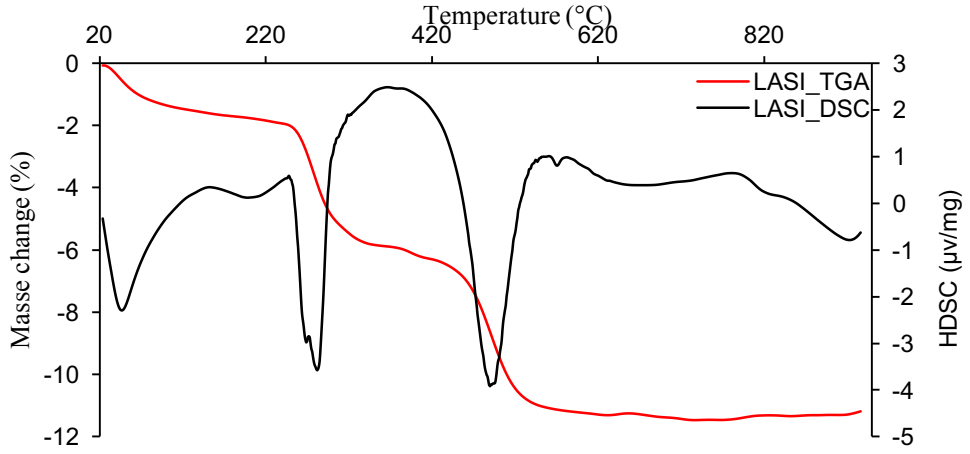

Figure 2 DSC thermogram and TGA curve of Laterite sample determined using a heating rate of 1 °C/min.

Kaolinite turns into metakaolinite by dehydroxylation. This dehydroxylation occurs at 493 ° C in our sample and leads to the conclusion that it would be disordered and therefore present a stacking defect in the crystalline plane [23, 24]. The endothermic peak around 570°C is related to the transformation of quartz α into β. The exothermic phenomenon around 955°C, to the structural reorganization of metakaolinite into a spinel phase [25]. The result of the TGA/DSC analysis is consistent with of the XRD's.

– ***Micrographic observations***

The morphology of raw laterite and heated laterite were investigated with SEM. **Figure 4** shows the textural change of laterite after thermal treatment at various temperatures. The laterite undergoes transformations during heating. In **Figure 4a**, the raw laterite is in the form of a compact matrix in which are included large sized figured elements compared to the constituents of the matrix, up to more than 250 µm in their largest dimension. The micrograph of the calcined laterite at 300°C shown in **Figure 4b**, shows several pores on the surface. These numerous pores would come from the departure of the hydroxyl groups of goethite as shown by [9] in their study on the effects of temperature on goethite. [21] by studying the mechanisms of transformation of goethite into hematite also found the appearance of micropores after calcination of goethite at 275°C.

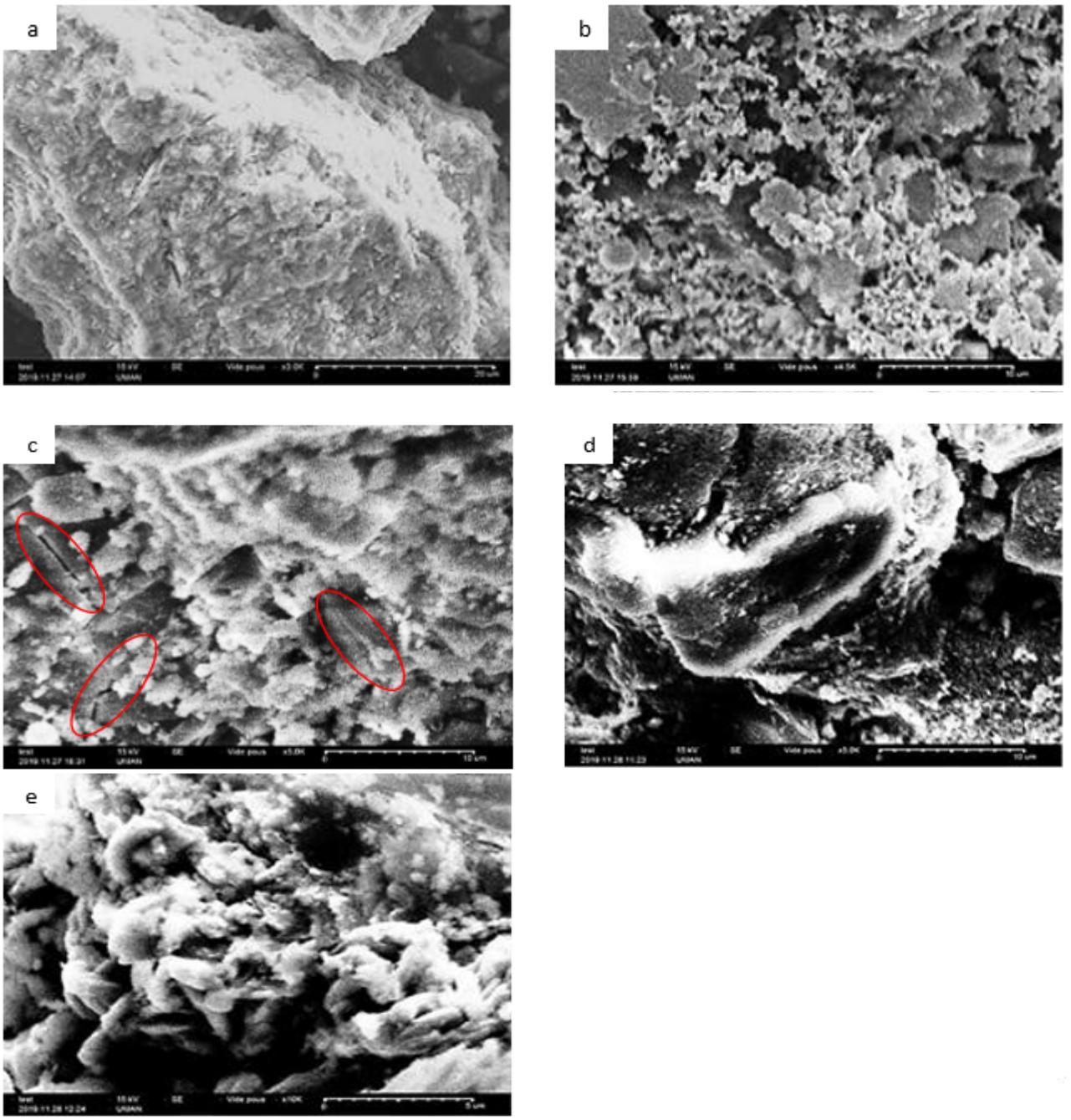

Figure 4. SEM micrographs of the laterite samples. a : Raw laterite ; b : heated laterite at 300°C ; c : heated laterite at 500°C ; d : heated laterite at 700°C et e : heated laterite at à 900°C during 2h.

Indeed, according to [9], micropores appear when the temperature is above 250°C the detail of this porosity is presented by Figure 5. Above 500°C, no obvious differences in morphology can be observed between Figure 4c-d-e. However, when observed under the high magnification SEM image, some subtle differences can be found between Figure 4c and the other two. From Figure 4c, it can be seen that small cracks appeared. This could be due to the fusion of the micropores giving mesopores around 400°C which finally becomes macropores around 600°C as reported by [9]. This fusion could be that of potassium oxide (K_2O), which has a melting point of 350°C.

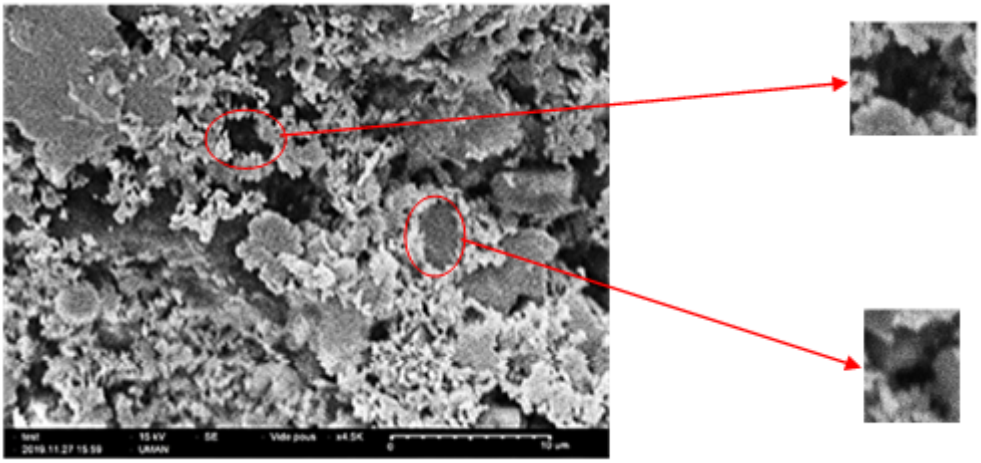

Figure 5. SEM micrograph of micropores on L300.

3.2 Phosphate retention on heat-activated laterites

– Solid / liquid ratio analysis

Looking for the best adsorbent mass/retention rate ratio has highlighted two steps in the retention of phosphates on heat-activated laterites (**Figure 6**). The first phase ranges from 0 to 12.5 g/L, 0 to 25 g/L, 0 to 37.5 g/L and 0 to 15 g/L for laterite calcined at 300°C, 500°C, 700°C and 900°C respectively. At this stage, the yield increases as the support mass grows until it reaches 96%, which is the maximum value for the first three materials (L-300, L-500 and L-700) and 68% for laterite L-900. This step is probably due to the increase in active sites and the specific surface area of laterites, which would promote the adsorption of large quantities of phosphate [26]. Beyond the observed maxima corresponding to the beginning of the second phase, the addition of adsorbent leads to a deposit in the reactors which results in an agglutination of the adsorbent particles. This aggregation of the particles causes a covering of the surfaces making the adsorption sites less available [2], hence the small variation in the retention rate for the L-300, L-500 and L-700 laterites. The progressive increase in the retention rate of L-900 laterite is thought to be due to the fact that the optimal dose has not yet been actually achieved despite the high dose of L-900 in solution. It would therefore make sense to set the optimal solid/liquid ratio of L-300 laterite at 5 g/L for phosphate retention. According to the same reasoning, the ratios found for laterites L-500 and L-700 are set at 7.5 g/L (yield = 84%) and 15 g/L (yield = 68%) for laterite L-900.

– Influence of stirring time

The adsorption of phosphates on the thermally activated laterites (L-300, L-500, L-700, and L-900) shows three-step kinetics (**Figure 7**), resulting in equilibrium in 6 h for the L-300 (qm = 0.32 mg/g of total phosphate), 8 h for L-500 and L-700 (qm = 0.31 and 0.3 mg / g of total phosphate respectively) and 12 h for L-900 laterite (qm = 0.29 mg / g of total phosphate). The first two phases show rapid growth in retention capacity with increasing reaction time, which testifies to the high reactivity of the four activated

materials. These two phases would in all likelihood be dependent on easily accessible sites such as the external surfaces of the particles and the macro-pores or would correspond to the fixation of phosphate ions on the most reactive sites (instantaneous adsorption). In fact, during calcination, the departure of water would lead to the development of macropores, significant porosity within the materials, and great accessibility to metal oxides and hydroxides. As for the last phase, slower, it would be characteristic of retention of the phosphates after diffusion of the ions in the meso- and micropores (gradual adsorption). This last phase represents the equilibrium phase.

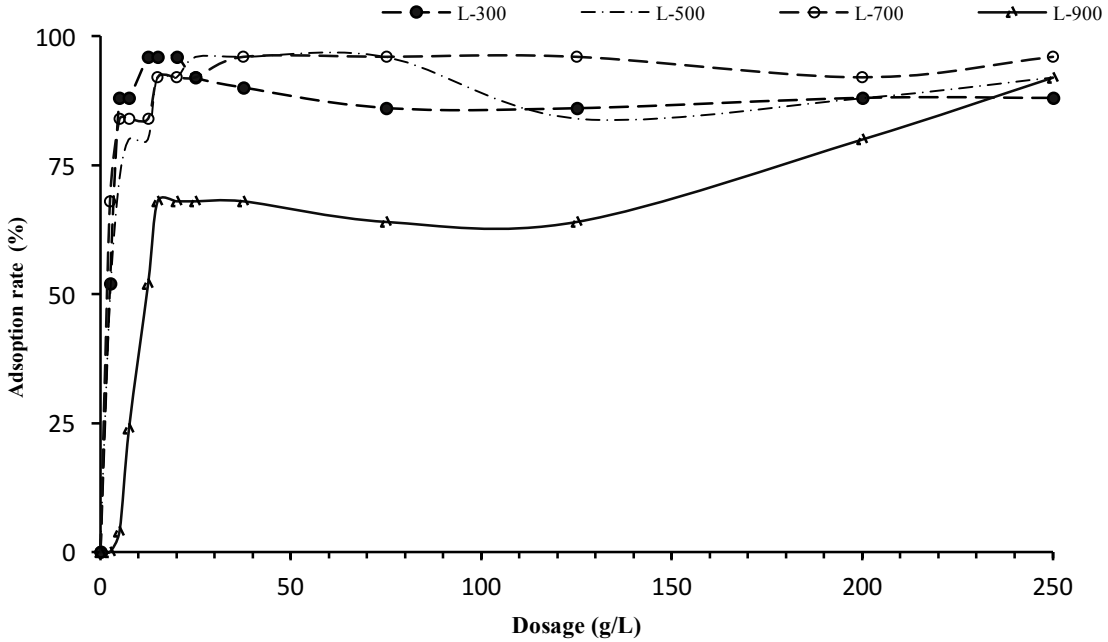

Figure 6. Effect of the mass of calcined laterite on phosphate removal rate. Initial P concentration = 5 mg/L; pH = 6 - 7; Temperature = 30°C.

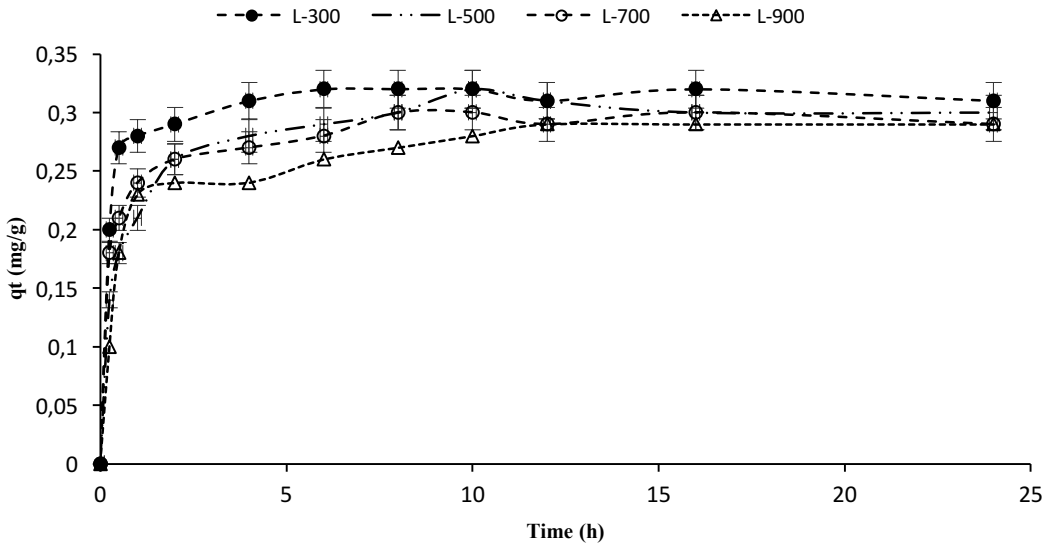

Figure 7. Contact time effect on phosphates adsorption by treated laterites: L-300, L-500, L-700 and L-900. Initial phosphate concentration = 5 mg / L; Solution volume = 100 mL, Stirring speed = 180 rpm; pH = 6 -7; Temperature = 30 °C.

– ***Influence of the initial concentration of P***

The investigation of the effect of different initial concentrations of P (2.5; 5 and 10 mg / L) on the efficacy of the treatment shows that the process of phosphate retention on the different supports is influenced by this parameter (**Figure 8**). For all calcined laterites, equilibrium retention capacities increase with increasing initial concentration and contact time. The orders of magnitude for L-300 laterite are 0.22; 0.32 and 0.66 mg / g of total phosphorus, for L-500 laterite of 0.22; 0.31 and 0.64 mg / g of total phosphorus, for L-700 laterite of 0.22; 0.3 and 0.63 mg/g of total phosphorus and finally for the L-900 laterite of 0.21; 0.29 and 0.63 total phosphorus for initial concentrations of 2.5; 5 and 10 mg/L respectively. This could be related to the increase in the concentration gradient as suggested for the interactions of fluoride with raw laterite by [27]. Indeed, the increase in phosphate ions in solution gives a greater chance of collision between them and the active sites. Moreover, one could observed that the same optima are reached for all the adsorbents, but the priming shows differences in the retention capacity (at the first hour of contact). This difference, which is better marked by the L-900 sample, could be associated with the morphological and mineralogical modifications due to the heat treatment.

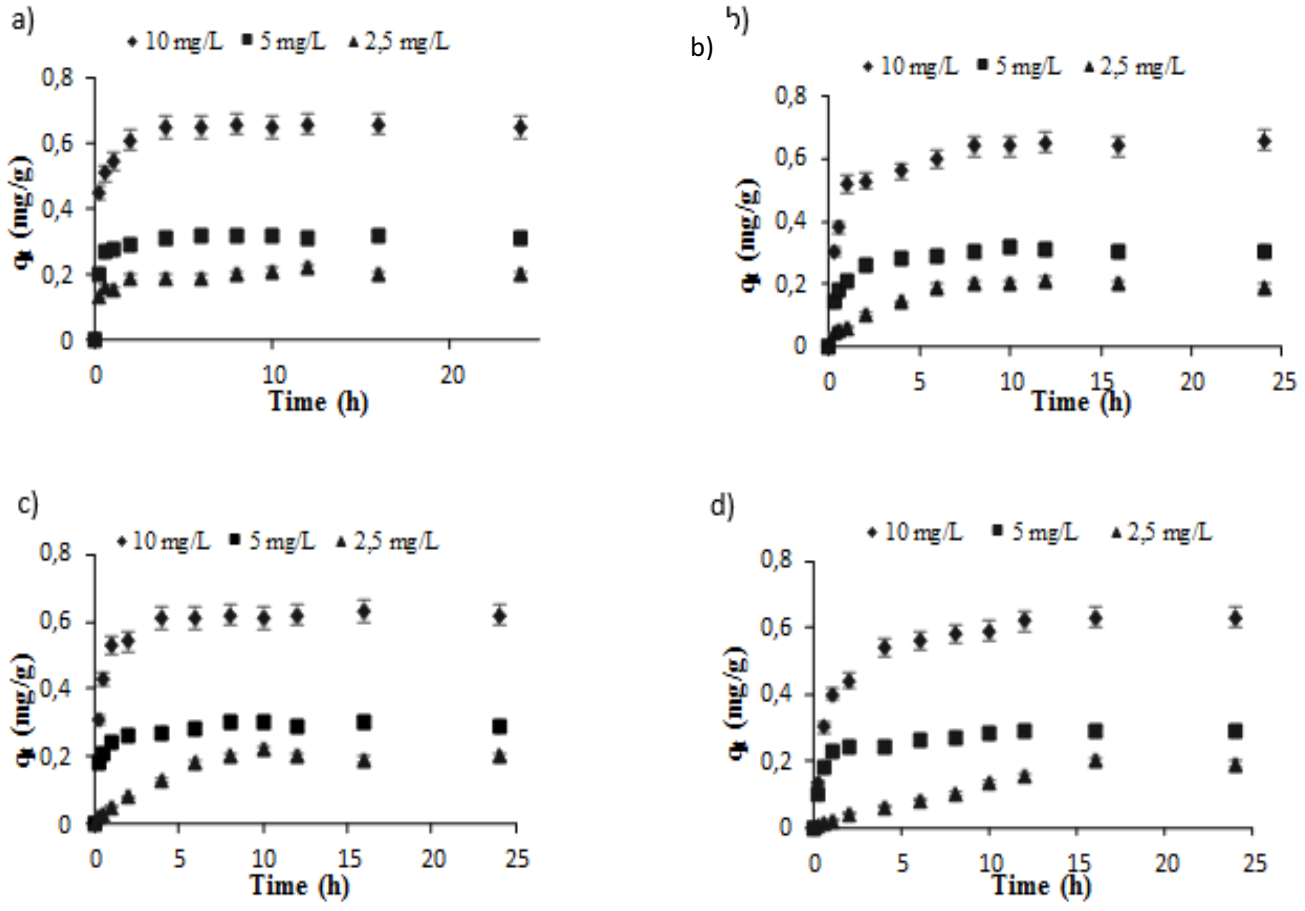

Figure 8. Effect of initial P concentration on phosphate adsorption by laterite L-300 (a), L-500 (b), L-700 (c) and L-900 (d). Initial concentrations: 2.5; 5; 10 mg/L; Volume of solution = 100 mL; Stirring speed = 180 rpm; pH = 6-7; Temperature = 30°C.

– ***Influence of pH***

The influence of the initial aqueous solution pH value as reported in **Figure 9**, show this parameter affects the phosphates adsorption process by laterite. For all thermally activated laterites, a decrease (low slope) in the rate of phosphate retention is observed as the initial pH of the solution is increased. The maximum retention ratio is obtained at pH = 2 with a value of 100, 92, 84 and 74% for the laterite L-300, L-500, L-700 and L-900 respectively. These results are probably due to the fact that in an acidic medium, the protonation process of the adsorption sites ($SOH + H^+ => SOH^{2+}$) provides a significant amount of positive charges on the surface of the adsorbents. Since the dominant species in this pH range are the anionic forms ($H_2PO_4^{2-}$ and HPO_4^-), adsorption easily occurs at adsorption sites through electrostatic interactions [12]. At pH=10, the minimum retention value is 72% for L-300, 68% for L-500, 64% for L-700 and 42% for L-900. Raising the pH of the adsorbate not only causes a large amount of negative charges on the surface of the adsorbents ($SOH => SO^- + H^+$) but also a high concentration of hydroxyl group in the reaction medium [28]. There would therefore be a competition between the negatively charged phosphate species and the hydroxyl groups on the positive adsorption sites still available and also a repulsion between the phosphate ions and the negatively charged sites. This would explain the gradual reduction in abatement rates down to pH = 10. Similar trends were observed by [29] with raw laterite.

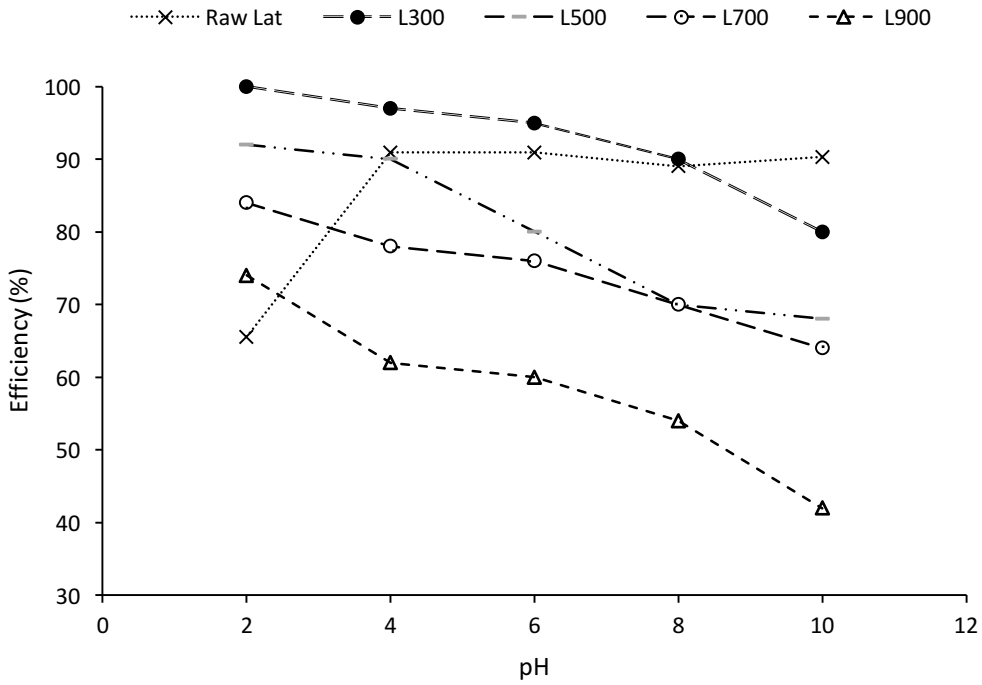

Figure 9. Effect of pH on the retention rate of phosphorus by calcined laterites: L-300, L-500, L-700 and L-900. Initial concentration: 5 mg/L; Volume of solution = 40 mL; Stirring speed = 180 rpm; Temperature = 30°C.

3.3 Modelling of the adsorption kinetics

The According to **Figures 10 ; 11** and **Table 1**, the application of the two surface reaction models when modelling adsorption kinetics, shows that the pseudo-second-order model better describes all of the experimental results due to the good similarity between the values of experimental q_e and those of q_e calculated from the model data. Moreover, the values of the correlation coefficients (R) are very close to 1. As for the Lagergren model (pseudo-first-order model), it does not agree with the experimental data

because the theoretical points obtained do not seem to follow a straight line. Otherwise, R values between 0.387 and 0.897 are relatively low. This shows that the transfer of phosphates cannot be described by a first-order law. In other words, the speed of the reaction does not depend solely on the concentration of phosphate in the solution. Compliance with the pseudo-second-order model suggests that chemisorption would be the dominant mechanism during the retention of phosphates on the four thermally activated laterites. Similar kinetics have been reported by [12] in a study of phosphates adsorption on activated laterite at 700°C. In addition, it was found that changes in the rate constant (k_2), seem to tend to decrease as the initial concentration increases. This would mean that this constant is closely related to the equilibrium concentration since the latter depends on the initial phosphate concentration [8].

Table 1. Kinetic parameters relating to pseudo-first-order and pseudo second-order models

Pseudo first-order model or Largergen model						Pseudo-second-order model			
activated laterites	C_0 (mg/L)	$q_{e,exp}$ (mg/g de P)	$q_{e\ cal}$ (mg/g de P)	k_1 (h^{-1})	R	$q_{e,exp}$ (mg/g de P)	$q_{e\ cal}$ (mg/g de P)	K_2(h^{-1})	R
L-300	**5**	0,321	0,020	0,118	0,486	0,321	0,320	11,200	0,999
L-500	**5**	0,310	0,041	0,070	0,387	0,310	0.307	12,164	0,999
L-700	**5**	0,300	0,060	0,089	0,714	0,300	0.296	22,388	0,999
L-900	**5**	0,290	0,102	0,240	0,897	0,290	0,295	7,492	0,999

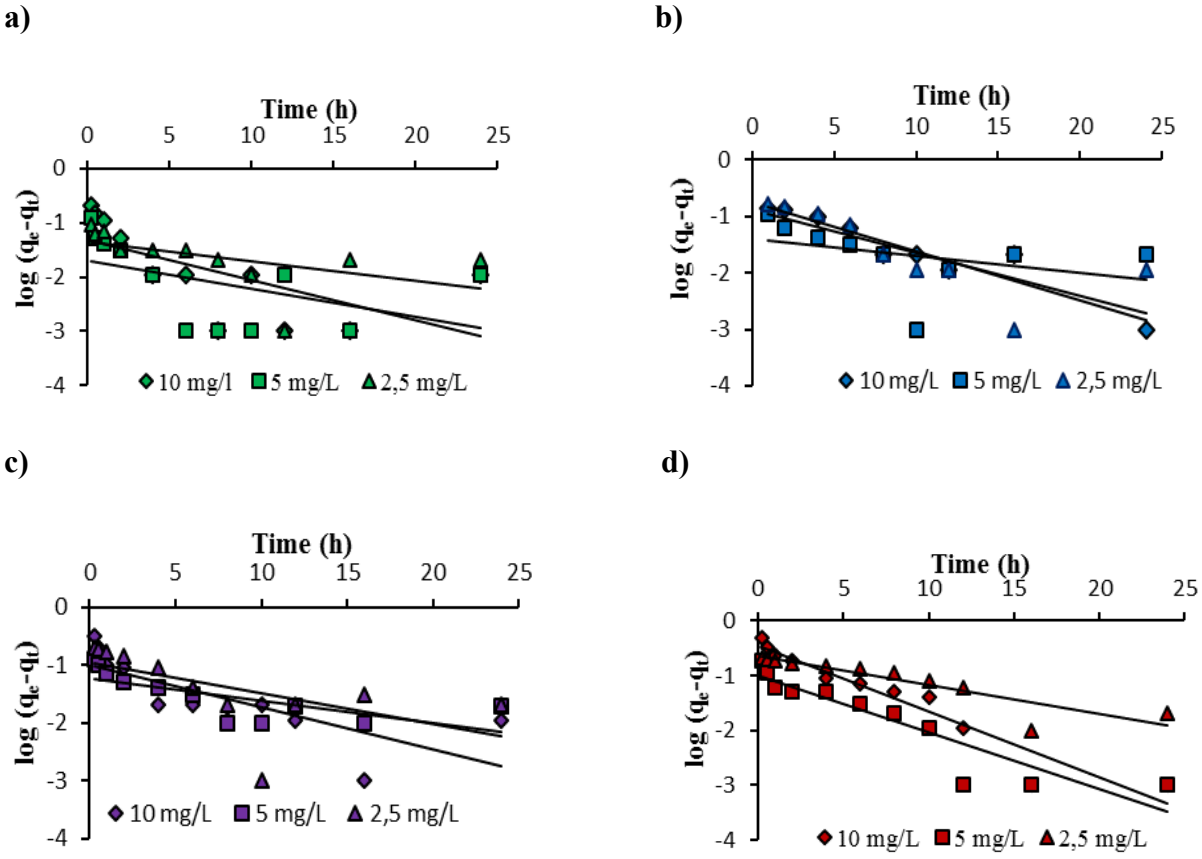

Figure 10. Pseudo-first-order model analyses for the phosphates adsorption onto calcined laterite (L-300 (a), L-500 (b), L-700 (c), and L-900 (d)) in solution of different initial concentration (2.5; 5 and 10 mgP/L).

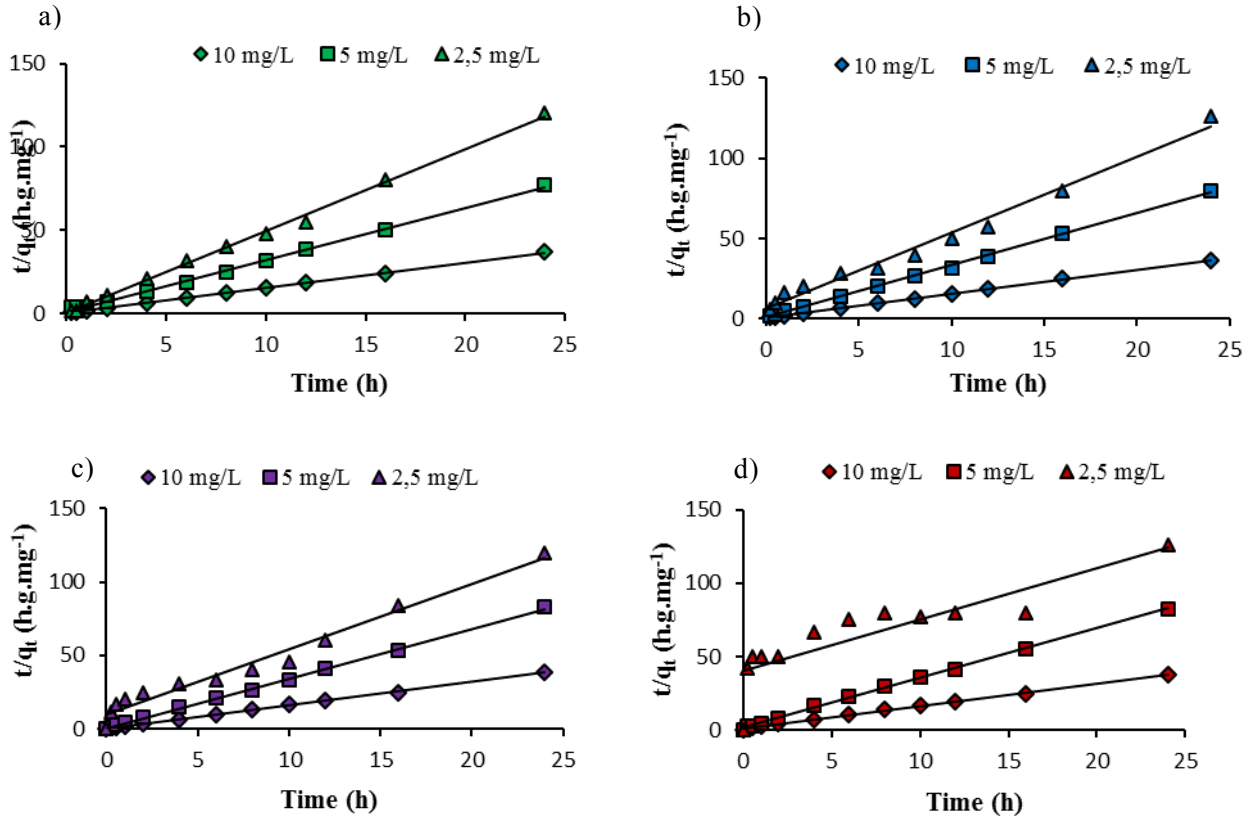

Figure 11. Pseudo-second-order model analyses for the phosphate adsorption onto calcined laterite (L-300 (a), L-500 (b), L-700 (c), and L-900 (d)) in solution of different initial concentration (2.5; 5 and 10 mgP/L).

3.4 Comparative study

The comparative study shows that the four thermally activated lateritic materials that served as phosphate retention support do not have the same capacities or the same efficiencies. Laterite activated at 300°C appears to be the best adsorbent for phosphates (**Figure 12**). The retention efficiency of calcined laterites can be classified according to the following sequence: L-300 > L-500 ≥ L-700 > L-900.

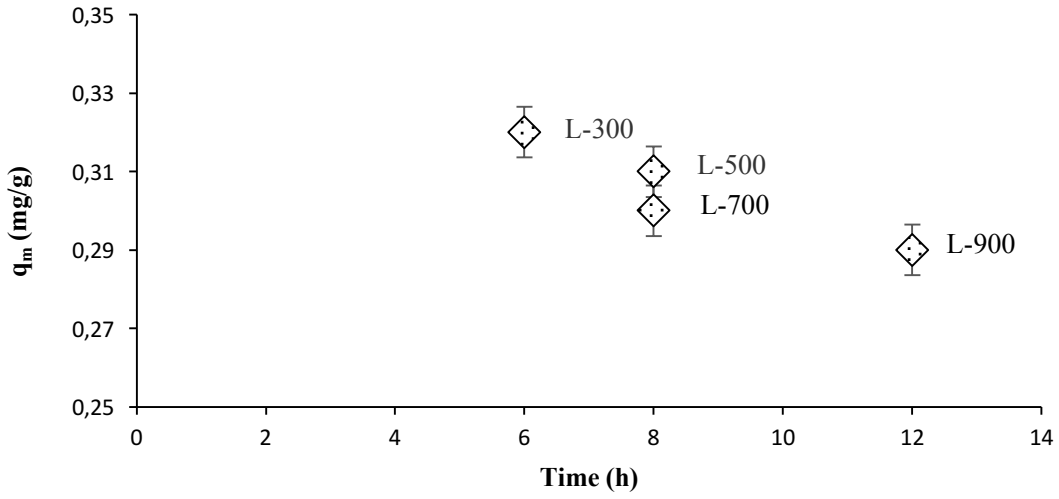

Figure 12. Distribution of adsorbents as a function of time and retention capacity.

The retention capacity of laterite calcined at 300°C probably results from the various transformations produced within the material during heating at this temperature. Indeed, the equilibrium time is short and the high adsorption capacity observed for L-300 could be due to the macropores developed during

the departure of water and to the presence of partially hydroxylated goethite also called proto-hematite and boehmite (partially dehydroxylated gibbsite), as demonstrated by the observations made with the SEM and the picks revealed by XRD diffractogram. Heating to 300°C would have induced the appearance of defects in the structure of the material, including voids formed by the departure of water and the formation of micropores. This mechanism has been demonstrated by [30]. Indeed, these authors have shown that partially dehydroxylated goethites consist of microporous mixtures of goethite and small sizes of hematite crystals with a larger specific surface area to promote significant adsorption compared to goethite and completely formed hematite. Heating to higher temperatures results in the reduction of the specific surface through the growth of hematite crystals and the reestablishment of structural defects (morphological reorganization) [31]. These observations would explain the decrease in the adsorption capacity with the increase in the calcination temperature, hence the reduction in the adsorbing power of the activated laterites at 500, 700 and 900°C. The results obtained with the treated laterite at 300°C are higher than those obtained with raw laterite during our previous work [8].

Conclusion

This work investigated the influence of thermal treatment of laterite on the removal of phosphates from domestic wastewater. Laterite materials heat-treated at 300° C (L-300), 500° C (L-500), 700° C (L-700) and 900°C (L-900) are all effective in retaining phosphates from water. For an initial phosphate concentration of 5 mg/L, optimal doses are 5 g/L for L-300, 7.5 g/L for L-500 and L-700 and 15 g/L for L-900. The kinetics study indicates that the optimal time required to reach equilibrium would be 6 hours for L-300, 8 hours for L-500 and L-700 and 12 hours of agitation for L-900. In addition, the process of phosphate adsorption by calcined laterites is highly dependent on the initial phosphate concentration and therefore on the equilibrium state of the system (adsorbate-adsorbent). Moreover, one could observed that the priming shows differences in the retention capacity according to Laterite treatment heat. The optimal pH retention is 2, for the four calcined laterites. Electrostatic (attraction/repulsion), chemical and/or ligand interactions would occur during phosphate retention by these four thermally activated materials. The highest correlation coefficients were obtained from the application of the pseudo-second order kinetic, thereby demonstrating that this model provided the best explanation and fit for the data obtained. This indicate, that chemisorption would therefore be the dominant mechanism during phosphate retention on the four thermally activated laterites. The comparative study shows that the phosphate retention efficiency of the four matrices with respect to phosphate ions, is in the order L-300, L-500, L-700 and L-900. The retention capacity and equilibrium time are higher in the order L-300, L-500, L-700 and L-900. In addition, the mass of support required (optimal dose) for phosphate removal is less for the L-300 than the other three activated laterites. The L-300 perform well as phosphate adsorbent compared to raw laterite found in the literature. Treatment with the heat-treated laterite at 300°C is therefore attractive and promotes efficient phosphate retention from wastewater.

Disclosure statement: *Conflict of Interest:* The authors declare that there are no conflicts of interest. *Compliance with Ethical Standards:* This article does not contain any studies involving human or animal subjects.

References

[1] M. Van der Perk "Soil and water contamination," Tailor and Francis group plc, London, UK, second edition. ISBN 9780415893435 (2012).

[2] S. L. Coulibaly, "Abattement des phosphates des eaux usées par adsorption sur des géomatériaux constitués de Latérite, grès et schistes ardoisiers," *Thèse de doctorat*, Université de Lorraine, France, (2014) 236 p.
[3] I. Bashir, F. A. Lone, R. A. Bhat, S. A. Mir, Z. A. Dar and S. A. Dar, "Concerns and Threats of Contamination on Aquatic Ecosystems," in *Bioremediation and Biotechnology.* Springer, (2020) 1-26.
[4] Q. Zeng, , L. Qin, L. Bao, Y. Li and X. Li, "Critical nutrient thresholds needed to control eutrophication and synergistic interactions between phosphorus and different nitrogen sources," *Environmental Science and Pollution Research*, 23 (2016) 21008–21019. doi:10.1007/s11356-016-7321-x.
[5] Y. Xu, Y. Dai, J. Zhou, Z. P. Xu, G. Qian, and G. Q. M. Lu, "Removal efficiency of arsenate and phosphate aqueous solution using layered double hydroxide materials: intercalation vs. precipitation," *Journal of Materials Chemisyty* 20 (2010) 4684–4691 https://doi.org/10.1039/B926239C.
[6] S. Hussain, H. A. Aziz, M. H. Isa, A. Ahmad, J. V. Leeuwen, L. Zou, S. Beecham, and M. Umar, "Orthophosphate removal from domestic wastewater using limestone and granular activated carbon," *Desalination* 271 (2011) 265–272.
[7] J. Mateo-Sagasta, S. M. Zadeh, H. Turral, J. Burke, "Water pollution from agriculture: a global review," FAO and IWMI (2017).
[8] L. S. Coulibaly, S. K. Akpo, J. Yvon and L. Coulibaly, "Fourier transform infra-red (FTIR) spectroscopy investigation, dose effect, kinetics and adsorption capacity of phosphate from aqueous solution onto laterite and sandstone," *Journal of environmental Management*, 183 (2016) 1032-1040
[9] J. Liu, Q. Zhou, J. Chen, L. Zhang and N. Chang, "Phosphate adsorption on hydroxyl–iron–lanthanum doped activated carbon fiber" *Chemical Engineering Journal*, 215–216 (2013) 859–867 doi:10.1016/j.cej.2012.11.067.
[10] Yu C. Z., J. Yang, L. A. Zhou, L. Z. Zhao, H. W. Zhang, J. N. Yin, G. F. Wei, K. Qian and Wang Y. H. "A designed nanoporous material for phosphate removal with high efficiency," *Journal of Materials Chemistry*, 21 (2011) 2489-2494 ; https://doi.org/10.1039/C0JM02718A.
[11] Y. Glocheux, M. M. Pasarín, A. B. Albadarin, C. Mangwandi, F. Chazarenc and G. M. Walker, "Phosphorus Adsorption onto an Industrial Acidified Laterite By–Product : Equilibrium and Thermodynamic Investigation," *Asia-Pacific. Journal of Chemistry Engineering*, 9 (6) (2014) 929-940, https://doi.org/10.1002/apj.1843.
[12] L. Zhang, W. Wu, J. Liu, Q. Zhou, J. Luo, J. Zhang and X. Wang, "Removal of phosphate from water using raw and activated laterite: batch and column studies," *Desalination and Water Treatment,* 52 (4-6) (2014) 778-783. doi:10.1080/19443994.2013.826786
[13] M. L. .Blanchet and L. Malaprade, "Méthode rapide de dosage des principaux éléments d'une roche silicatée," *Chimie analytique* 4 (1) (1967) 11-26.
[14] J. Kim, G. Dodbiba, H. Tanno, K. Okay, S. Matsuo and T. Fujita, "Calcination of low-grade laterite for concentration of Ni by magnetic separation" *Minerals Engineering,* 23(4) (2010) 282-288.
[15] B. K. Gan, I. C. Madsen and J. G. Hockridge, "In situ X-ray diffraction of the transformation of gibbsite to [alpha]-alumina through calcination: effect of particle size and heating rate," Journal of Applied Crystallography, 42 (2009) 697-705 doi:10.1107/s0021889809021232
[16] V. J. Ingram-Jones, R. C. T. Slade, T. W. Davis, J. C. Southern and S. Salvador. "Dehydroxylation sequences of gibbsite and boehmite : Study of differences between Soak and flash calcination and of particle-size effects" *Journal of Materials Chemistry*, 6 (1) (1996) 73-79.

[17] P. L. Huestis, T. R. Graham, S. T. Mergelsberg and J. A. LaVerne, "Identification of Radiolytically-Active Thermal Transition Phases in Boehmite," *Thermochimica Acta*, 689 (2020), 178611. https://doi.org/10.1016/j.tca.2020.178611
[18] S. E. Olsen, M. Tangstat and T. Lindstad, Production of Maganese Ferroalloys, Tapir Akademisk Forlag Trondheim, ISBN 9788251921916 (2007).
[19] Y. Wang and W. J. Thomson, "The effects of steam and carbon dioxide on calcite decomposition using dynamic X-ray diffraction," *Chemical Engineering Science*, 50(9) (1995) 1373–1382. doi:10.1016/0009-2509(95)00002-m
[20] Y. Sakai and N. Koga, "Kinetics of component reactions in calcium looping appeared during the multistep thermal decomposition of Portland cement under various atmospheric conditions" *Chemical Engineering Journal*, 428 (2022) 131197 https://doi.org/10.1016/j.cej.2021.131197.
[21] F. Jia, K. Ramirez-Muñiz, and S. Song, "Mechanism of the formation of micropores in the thermal decomposition of goethite to hematite" *Surface and Interface Analysis*, 47 (2015) 535–539.
[22] A. Longos, A. A. Tigue, R. A. Malenab, I. J. Dollente and M. A. Promentilla, "Mechanical and thermal activation of nickel-laterite mine waste as a precursor for geopolymer synthesis," *Results in Engineering*, 7 (2020) 100148. doi:10.1016/j.rineng.2020.100148
[23] P. R. Uitch, "Mechanism for the Dehydroxylation of Kaolinite, Dickite, and Nacrite from Room Temperature to 455°C," *Journal of the American Ceramic Society*, 69 (1), (1986) 61–65. doi:10.1111/j.1151-2916.1986.tb04695.x
[24] J. Kloprogge, "Thermal, Mechanical and Chemical Treatments of the Kaolin Minerals" *Springer Mineralogy*, 161–241 (2018), doi:10.1007/978-3-030-02373-7_5
[25] Y. Millogo, Etude géotechnique, chimique et minéralogique de matières premières argileuses et latéritiques du Burkina Faso améliorées aux liants hydrauliques : Application au génie civil (bâtiment et route), Thèse de doctorat, Université de Ouagadougou, Burkina Faso, (2008), 144 p
[26] M. Mourabet, H. E. Boujaady, A. E.Rhilassi, H.Ramdane, M. Bennani-Ziatni, R. E. Hamri and A. Taitai, "Defluoridation of water using Brushite : Equilibrium, kinetic and thermodynamic studies" *Desalination,* 278(1) (2011) 1-9.
[27] M. Sarkar, A. Banerjee, P. P. Pramanick and A. R. Sarkar, "Use of laterite for the removal of fluoride from contaminated drinking water" *Journal of Colloid Interface Sciences*, 302(2) (2006) 432-441.
[28] J. Y. Liu, L. Zhang, L. H. Wan, N. Chang, C. Duan, Q. Zhou, X. L. Li and X. Z. Wang, "Removal of phosphate from water by activated carbon fiber loaded with lanthanum oxide," *Journal of Hazardous Materials*, 190 (2011) 848-855.
[29] R. S. Vyshak and S. Jayalekshmi, "Soil – an adsorbent for purification of phosphate contaminated water," *International Journal of Structural and Civil Engineering Research*, 3(2) (2014) 66-78.
[30] H. D. Ruan and R. J. Gilkes, "Kinetics of phosphate sorption and desorption by synthetic aluminous goethite before and after thermal transformation to hematite" *Clays Clay Minerals,* 31(1) (1996) 63-74
[31] H. D. Ruan and R. J. Gilkes, "Dehydroxylation of aluminous goethite: unit cell dimensions, crystal size and surface area" *Clays Clay Mineral*, 43 (2) (1995) 196-211.